Analyst

ROYAL SOCIETY OF CHEMISTRY

PAPER

View Article Online
View Journal | View Issue

Cite this: *Analyst*, 2025, **150**, 1140

Shifted-excitation Raman difference spectroscopy and charge-shifting detection coupled with spatially offset Raman spectroscopy for heritage science†

Alberto Lux, *[a,b,c] Claudia Conti, [a] Alessandra Botteon,[a] Sara Mosca [c] and Pavel Matousek *[a,c]

In situ measurements have great importance since in many scientific fields certain samples cannot be moved because of diverse reasons (excessive dimensions or weight, security, logistics *etc.*). In heritage science, this is a crucial requirement due to the high value of art objects, requiring non-invasive and *in situ* analyses. Therefore, it is important to have analytical methods capable of providing relevant information also outside laboratory environments. Such measurements face multiple challenges: for example, interference from ambient light or formation of artefacts due to undesired motions of the instruments. In Raman spectroscopy, a number of solutions have been demonstrated to mitigate these effects. For instance, Shifted Excitation Raman Difference Spectroscopy (SERDS) has proven efficient in removing the fluorescence of the sample and ambient light interference, and a charge-shifting detection approach was shown to be valuable in dealing with varying ambient light. In this study, we provide a comparison of conventional Raman spectroscopy, Shifted Excitation Raman Difference Spectroscopy (SERDS), charge-shifting detection technology and a combined SERDS and charge-shifting approach, in order to evaluate their effectiveness in mitigating fast evolving interfering backgrounds (*e.g.*, varying ambient light). Further investigations were also carried out into the potential of coupling of these methods with Spatially Offset Raman Spectroscopy (SORS) to facilitate more effective non-invasive investigations of subsurface sample components (*e.g.* paint layers). The study was carried out using samples mimicking cultural heritage materials with different degrees of complexity and in the presence of fluorescence and ambient light interference. The results are, nevertheless, applicable more generally to other areas such as forensics or biomedical fields, where both dynamic and static interferences can hinder measurements.

Received 1st October 2024,
Accepted 31st January 2025

DOI: 10.1039/d4an01280a

rsc.li/analyst

Introduction

The removal of fluorescence and ambient light from Raman spectra is of great importance in many application areas including forensics,[1–3] biomedical field,[4,5] food[6] or heritage science,[7] especially in cases where *in situ* measurements are required, for example, due to security reasons, inability to move the sample or logistics issues. In this context, many solutions have been developed in the past few decades to deal with such scenarios. These include Shifted Excitation Raman Difference Spectroscopy[8–11] (SERDS) and charge-shifting detection (CS). The specifics of the working principles of SERDS[8,12–14] and charge-shifting[15–17] are detailed in previous works: briefly, SERDS employs two excitation laser wavelengths that possess a very narrow wavelength difference, on the scale of bandwidths of Raman bands present, and since the fluorescence and ambient light background signals remain constant, whereas Raman signals shift with the corresponding amount, a subtraction of the pair of spectra obtained with each excitation wavelength effectively removes fluorescence and ambient light.[15–17] However, difficulties may arise when the background interference is not static but varies in some manner (such as due to fluorescence bleaching,[18] variation of ambient light intensity, the passing of a cloud in outdoor measurements or the shadow cast by the operator onto the instrument during acquisition) as SERDS is not able to deal with background intensity changes taking place between the

[a]*Institute of Heritage Science, National Research Council (CNR-ISPC), Via Cozzi 53, 20125 Milan, Italy. E-mail: alberto.lux@mail.polimi.it*
[b]*Sapienza University of Rome, Faculty of Literature, Department of Classics, Piazzale Aldo Moro 5, 00185 Rome, Italy*
[c]*Central Laser Facility, Research Complex at Harwell, STFC Rutherford Appleton Laboratory, UK Research and Innovation (UKRI), Harwell Campus, OX11 0QX, UK*
† Electronic supplementary information (ESI) available. See DOI: https://doi.org/10.1039/d4an01280a

two consecutive acquisitions at the two different excitation wavelengths. To address this issue, charge-shifting (CS) technology offers potential advantages: it employs an adapted CCD that receives signals illuminating only certain rows on its chip with alternating blocks of rows being unilluminated. In conjunction with rapidly alternating switching between the two excitation wavelengths, or between ON and OFF states where only one laser wavelength is used, the charges are shifted in synchrony up or down between the illuminated and obscured zones.[15] After the acquisition, by subtracting the incoming signals of the two different sets of rows, it is possible to reject the dynamic interference of ambient light, since the frequency at which the charges are shifted can be much higher (1–10 kHz)[17] than the typical frequency of the considered background variations. However, charge-shifting alone is not able to deal with the static component of sample fluorescence, which is the reason for its coupling with SERDS. Moreover, the employment of SORS[19] with said technologies paves the way also for the investigations of subsurface layers of materials in a non-invasive manner, in addition to the rejection of both static and dynamic interference backgrounds.[20–22] In this study, we evaluate the capabilities and limitations of these methods applied to cultural heritage samples. The samples were selected for their intrinsic complexity and challenges (*e.g.* Raman scattering efficiency and fluorescence). The experiments were further challenged by carrying out these measurements under dynamically varying ambient light to mimic *in situ* conditions, combining and comparing these techniques for the first time.

Materials and methods

Set-up

The experimental set up used in this study is based around a custom-built SORS system described in detail in previous publications.[16,17] Its schematic diagram is shown in Fig. S1 of the ESI.† Briefly, the system is a SORS point-like excitation–collection system that utilizes a purpose-designed integrated SERDS laser module[23] emitting at λ_1 = 829.40 nm (L1) and λ_2 = 828.85 nm (L2). The laser spot size and the collection area diameters are ~500 μm and ~1.5 mm, respectively. The SORS spatial offset is achieved by moving the entire collection path assembly with a motorized stage (MTS25-Z8 with a KDC101 controller, Thorlabs). The collected Raman signal is then sent to an imaging spectrometer (HoloSpec f/1.8i, Kaiser Optical Systems) coupled with a custom-made charge-shifting CCD (DU420A-BR-DD-9UW, Andor Technology). A custom made micro-machined metal mask, placed at the entrance slit of the spectrograph, made out of a tungsten foil (thickness = 100 μm, lateral dimensions: 10 mm × 5 mm, grid dimensions: height = 6 mm, width = 3 mm), was employed to shield (with a periodical pattern corresponding to CCD 8-pixels ON and OFF) the CCD sensor along the vertical axis, as required for the CS method.[17] Raman measurements were performed both at 0 mm (*i.e.* imaged) and 2 mm spatial offsets. Laser intensity and acquisition times were adjusted to attain equivalent illumination conditions (the overall laser energy delivered to the sample, in multiple pulses and per measurement, was set to ~2.1 J) in all the charge-shifting, SERDS and conventional acquisition modalities (a detailed schematic diagram is shown in Fig. S2 of the ESI†). An overview of experimental parameters for conventional, SERDS and CS read-out modalities is provided in Table 1. The wavelength calibration (pixel to relative Raman shift) was carried out using an aspirin tablet (using laser L1). To improve comparison between techniques, signal-to-noise ratios (S/N) have been added in the captions of the figures, calculated using the method described by Mosca *et al.*[24] where the noise is assumed to be the largest artefact present in the spectra or photon shot noise amplitude, whichever is greater. In the case of SORS measurements, only ratios relative to the offset spectra have been computed assuming that the bottom layer signal is the signal of interest.

Table 1 Overview of experimental parameters for the different readout modalities to attain ~2.1 J on the sample over the measurement time

Modalities		Average power (mW)	Time (s)
Conventional (L1)		60	35
SERDS	L1	60	17.5
	L2	60	17.5
CS (L1 only)		30	70
CS + SERDS	L1	60	35
	L2	60	35

Acquisition modalities and post-processing

Conventional. Spectra were initially acquired in conventional mode using laser L1, with a laser power equivalent to 60 mW and acquisition time set to 35 s (which confers to the sample an overall energy of 2.1 J per measurement, as shown in the schematics in Fig. S2†).

SERDS. Similar to the conventional method, spectra with L1 and L2 were collected one after the other. The same laser power was employed for both lasers and acquisition time was halved to 17.5 s, so that the overall energy was equal to the conventional measurements. Difference spectra were obtained by subtracting the two Raman spectra obtained at the two respective excitation wavelengths. Additionally, reconstructed SERDS spectra were calculated using a reconstruction algorithm developed in Python, based on previous work.[25] The routine is particularly basic, considering that our aim was to show how many artefacts might appear due to background interferences and how much effort would be required to design and implement a suitable routine to remove them all. Instead, employing a suitable combination of techniques and approaches might resolve the issue at its root. Moreover, removing narrow room light bands becomes even more complicated for in-field instrumentation, as the resolution of these spectrometers is comparable with the Raman bandwidths (as is typical of these devices, in order to maximise light throughput) and consequently the interfering emission lines have comparable widths with Raman bands: as such, their differentiation from Raman signals is not straightforward. Additional

subtraction of polynomial backgrounds could further improve the outcomes in a number of cases. We have not performed this correction here to retain background distortions present as they enable the most direct comparison between the performances of individual techniques.

CS. The system was operated at 1 kHz. The timing and synchronization between the laser wavelengths and the charge-shifting CCD read-out were controlled by a digital delay generator (DG645, Stanford Research Systems) connected to the laser driver module and external CCD trigger (further details can be found in our previous study[15–17]). The trigger voltage value for each laser was adjusted to provide an average power of 30 mW at the sample in a 50% duty cycle mode. The equivalent acquisition time was set to 70 s (laser pulse width (T_w) × number of cycles × number of repetitions). It is worth underlining that we operated the charge shifting instrument at 50 000 numbers of cycles (maximum possible value for CS cycles – additional details are given in the ESI in Fig. S3 and 4†) to achieve the desired overall energy on the sample, equal to those from the other techniques. Thus, we accepted that some degree of charge leakage between alternating CCD rows could occur,[17] adding some extra noise-like features to the spectrum.

Samples

The samples were chosen with increasing complexity in order to challenge the techniques at different levels. We started with a standard non-fluorescent sample and then moved on to more realistic, fluorescing ones.

• S0 – a sample consisting of polytetrafluoroethylene (PTFE), about ~8 mm thick and roughly 4 × 4 cm wide, used as a standard non-fluorescent sample.

Single layer measurements:

• S1 – phthalocyanine blue ($C_{32}H_{16}N_8Cu$), a common pigment used in art, painted on a wooden support. This sample was collected from an atelier in Milan, which refused citation. It was effectively a single layer system since the Raman signal from the substrate was undetectable. In this case, phthalocyanine blue paint was highly absorbing and fluorescing. The blue layer was about 10 μm thick and roughly 5 × 5 cm wide.

• S2 – a gypsum ($CaSO_4{\cdot}2H_2O$) layer, cut from a solidified mixture of gypsum powder and water, mimicking a plaster, stucco or preparation layer for paintings. Preliminary spectra showed some fluorescence signal from this sample. The sample was 0.5 mm thick and 2 × 5 cm wide, and was prepared in ISPC laboratory in Milan.

• S3 – a calcite ($CaCO_4$) layer, often employed as plaster or a preparation layer for paintings, applied on paper (the latter did not provide any Raman signal). This sample was not prepared in our laboratory, but instead was acquired from the atelier in Milan mentioned above. Also, in this case only the calcite signal (top layer) from the preparation layer was detected, along with fluorescence possibly originating from the paper. The whole sample is about 1 mm thick and 5 × 5 cm wide.

The first four samples (S0, S1, S2, S3) were all analysed on the front and on the back sides. The only samples that showed any difference between the front and back signals were the S1 sample, which, as already mentioned, did not provide any signal from the wooden substrate, and the S3 sample, where the preparation layer was likely applied only on one side of the paper.

SORS measurements:

• S4 – a thin tape of PTFE (0.25 mm thick) placed on top of a marble support, which itself yields a strong calcite Raman

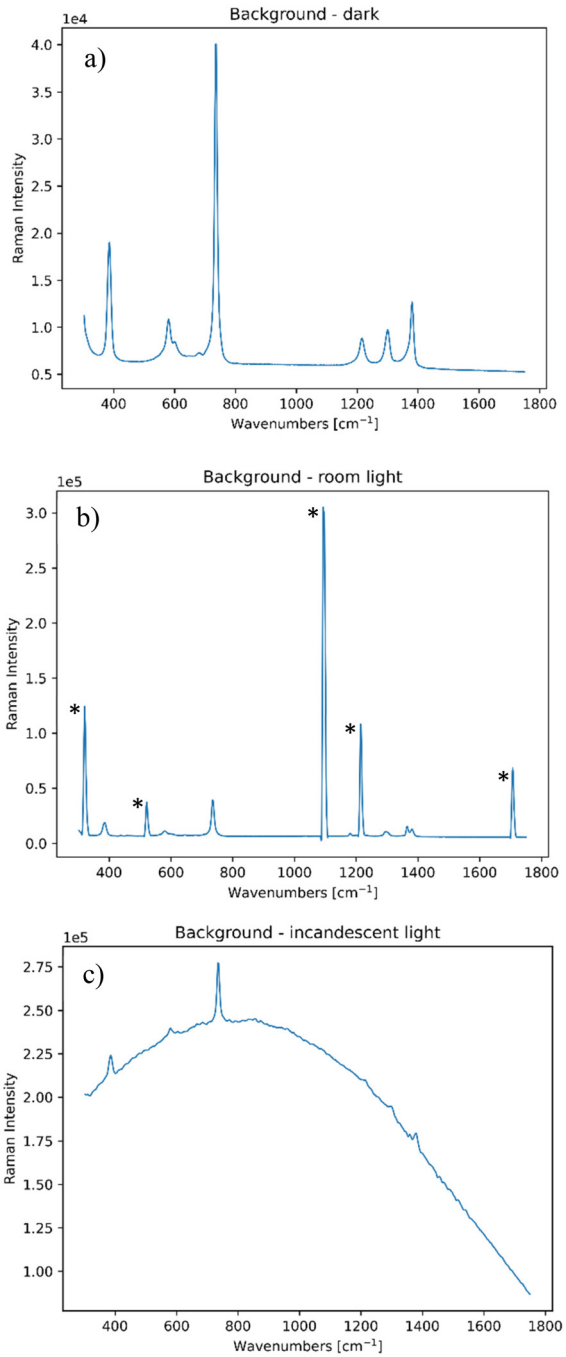

Fig. 1 Standard PTFE spectrum collected (a) in the dark; (b) in the presence of a room ceiling light and (c) in the presence of an incandescent lamp. All these spectra have been collected at zero spatial offset.

signal. Both layers possessed appreciable Raman scattering efficiency and a very small degree of fluorescence.

• S5 – the sample was created using a block of PTFE as a substrate (8 mm thick) and S3 used as the top layer.

S4 and S5 samples mimic contemporary art and design materials (plastics) or collages.

All samples were analysed with room light with an additional incandescent light being present. Dynamic variation of these emission sources was achieved by a random pattern hand waving between the emission sources and the sample. More details are given in the following section.

Results and discussion

Ambient light interference

In order to be able to mimic both static and dynamic interferences, two ambient light sources were employed, namely a room ceiling lighting of the laboratory, which consisted of fluorescent lamps that had narrow bands at around 852, 912, 922 and 966 nm (equivalent to 320, 1093, 1215 and 1706 cm^{-1} and highlighted by asterisks in Fig. 1), and a broadband light source consisting of a 35 W halogen bulb (*i.e.* incandescent light) that emitted black body radiation to simulate sun type of radiation. Their impact on a standard Raman spectrum of PTFE is shown in Fig. 1.

It is important to note that all these contributions are static, and so one needs to implement a dynamic contribution to these, in order to provide a random variation of the background light to mimic the above discussed non-static situations encountered in field measurements. We mimicked a common situation of passing of a cloud in front of the sun by randomly obstructing the incandescent light with different degrees of hand coverage. The random occurrence of shadows covering the room light was simulated by moving a hand in an irregular fashion, so to slightly obstruct its incoming ceiling room light radiation on the collection side.

Standard sample (S0). We initially analysed a standard PTFE sample to assess the impact of the different light sources on a non-fluorescent sample. Conventional Raman spectra (Fig. 2a) yield a discernible Raman signal of PTFE (highlighted with the letter R), mostly due to the high scattering efficiency of PTFE.

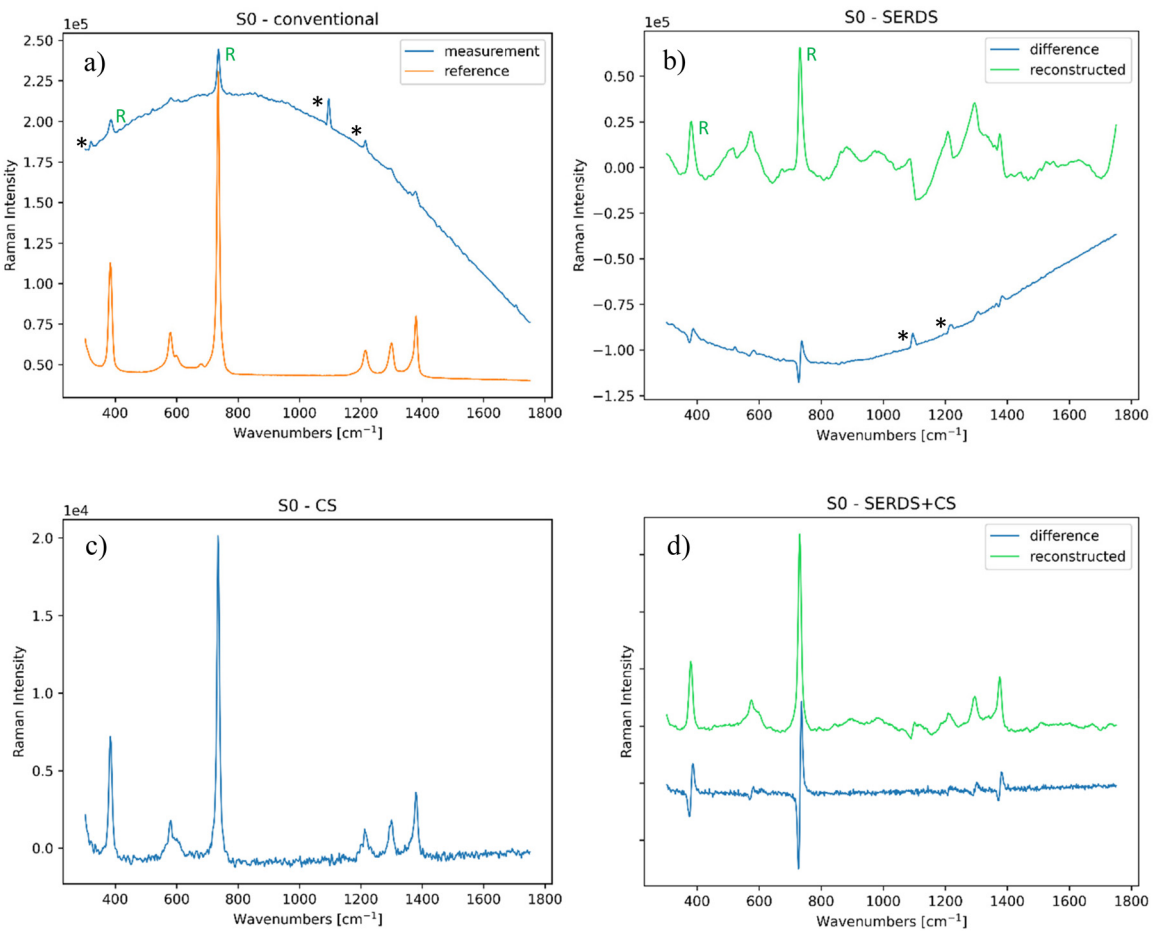

Fig. 2 (a) Conventional Raman spectrum of the PTFE sample, compared with the reference PTFE spectrum (S/N = 1.9); (b) SERDS measurement of the same sample (S/N = 2.1); (c) CS measurement of the same sample (S/N = 89); (d) SERDS + CS measurement of the same sample (S/N = 82). The bands highlighted with (*) are ambient light artefacts, the ones with (R) in a and b are the most intense PTFE Raman bands. All these spectra were analysed at zero spatial offset.

However, the spectrum is strongly contaminated with spurious background light bands (identified by asterisks). Fig. 2b shows both reconstructed (green line) and difference (blue line) spectra of a SERDS measurement, which could remove most of the fluorescence interference but not completely, as it struggled to suppress its dynamically varying component. Consequently, the interfering sloping background dominates the PTFE Raman signal with strong room light emission bands being also present. It is interesting to compare the different behaviours of SERDS with a static or dynamic background interference, as shown in Fig. S5 in the ESI:† indeed the technique is perfectly able to remove any static ambient light, but struggles when its variation is involved. As specified above, the reconstructing routine is rather basic in order to show how invasive the presence of artefacts would be with the minimum effort to remove them, as the complete clean removal would be relatively demanding with respect to rejecting any interference directly during the measurement. CS measurement with L1 only (Fig. 2c) yielded a comparable Raman spectrum with respect to that of CS + SERDS (Fig. 2d): this is due to the low amount of fluorescence emitted by the sample rendering the employment of SERDS non-essential in this situation.

Single layers

In the first part of this study, we considered single layer samples before moving to more complex ones such as multilayer systems where SORS was additionally deployed.

Painting layer (S1). A sample of a phthalocyanine blue painting layer applied on a wooden support was selected to study the performance of the techniques on a typical cultural heritage sample. The paint is highly absorbing and fluorescing, making the detection of its characteristic Raman bands (among the strongest, 749 and 1527 cm^{-1} are underlined) challenging at times. As stated earlier, the Raman signal from the support layer was not detected due to the high phthalocyanine absorption at the excitation wavelengths. Fig. 3a shows the conventional Raman measurement (blue line) compared with the pigment reference spectrum (orange line). In this case, it is not straightforward to distinguish S1 Raman signatures since the conventional Raman spectra are dominated by background interferences. In contrast, SERDS measurement was able to distinguish it through its characteristic 'derivative-like' shape (see Fig. 3b – highlighted with an orange ellipse). However, even in this case, SERDS spectra are still dominated by ambient light spectral artefacts,

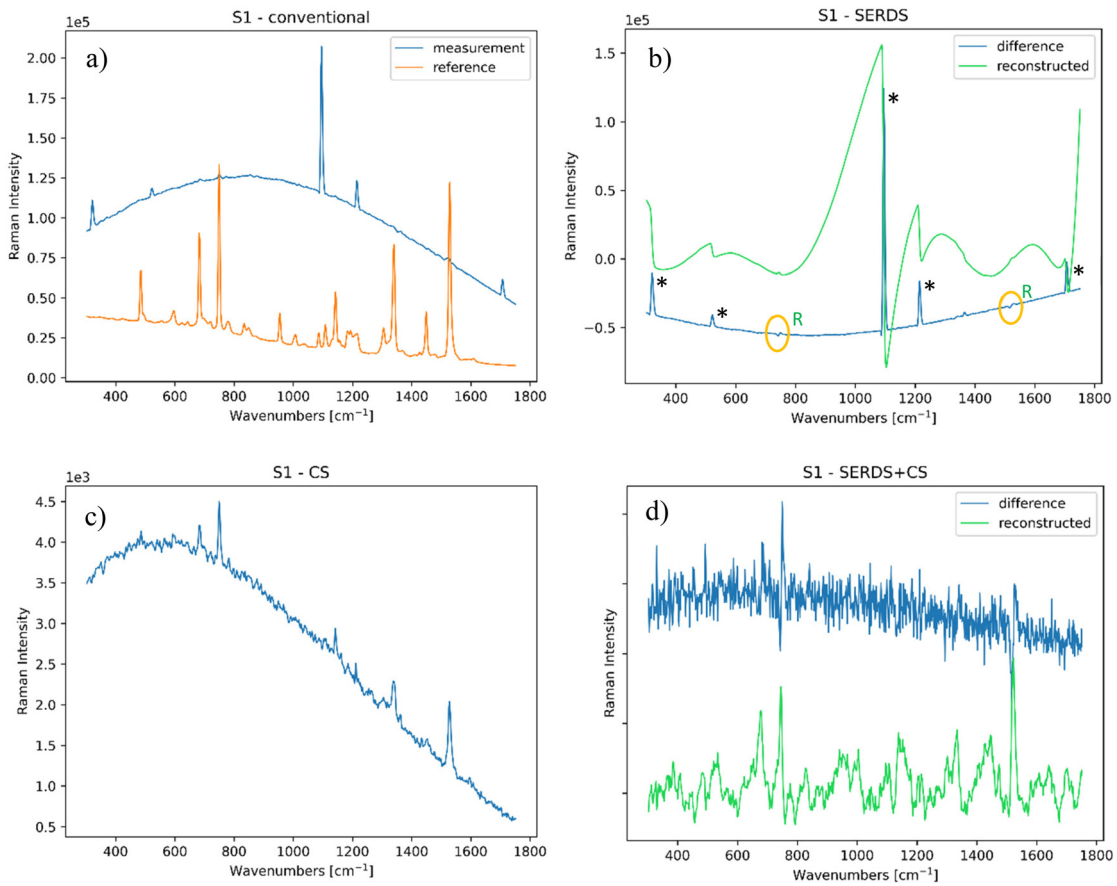

Fig. 3 (a) Conventional Raman spectrum of the BW sample, compared to the reference (S/N = 0.1); (b) SERDS measurement of the same sample (S/N = 0.01). Bands highlighted with (R) are S1, more intense Raman bands; (c) CS measurement of the same sample (S/N = 14); and (d) SERDS + CS measurement of the same sample (S/N = 4). All bands highlighted with (*) are artefacts or background interferences.

especially when reconstructed with a basic routine: particularly the narrow bands of the room light, when integrated, provide highly interfering artefacts – this is due to both the elevated variation of the room light intensity during the measurement and the consequential integration of a band that has no "derivative-like" shape as the SERDS signal, which leads to the generation of a fictitious derivative-like band by applying the reconstruction algorithm. This outcome was found more than once in our spectra, as the reconstruction routine employed was rudimentary and not attempting to filter out any similar features, as explained also in the Materials and methods section. In contrast, the charge-shifting measurement (see Fig. 3c) yielded much better results being able to completely remove the dynamic background interferences and as such to detect clearly the characteristic Raman bands of the paint. However, the spectrum still possessed a characteristic sloping background due to the fluorescence emitted from the sample. This sloping background was then suppressed by the SERDS + CS measurement (see Fig. 3d), although the spectrum exhibited a higher degree of noise (this is attributed to operating the charge shifting instrument at a higher number of cycles than the optimal one, as explained above).

Gypsum (S2). Another relevant compound from a cultural heritage standpoint is gypsum. It is typically found as degradation product in brickworks or employed in the preparation layer of paintings and in stuccos, and has a characteristic band at around 1007 cm^{-1}. The conventional Raman measurement shown in Fig. 4a along with a reference spectrum of gypsum (obtained with no ambient light) evidences a weak Raman signal overwhelmed by ambient light spectral features. As expected, SERDS measurement struggled with the dynamic variation of ambient light too, with the Raman signal of gypsum still dominated by ambient light artefacts (Fig. 4b). Indeed, the narrow room light band is seen as a Gaussian peak, which means that performing the reconstructing routine (which is basically an integration procedure) gives a raising slope at the artefact frequency. In contrast, the charge-shifting method performed much better (Fig. 4c): the strong Raman band is clearly visible, and ambient light contributions are effectively removed this time. However, a high sloping background is still present due to fluorescence emanating from the

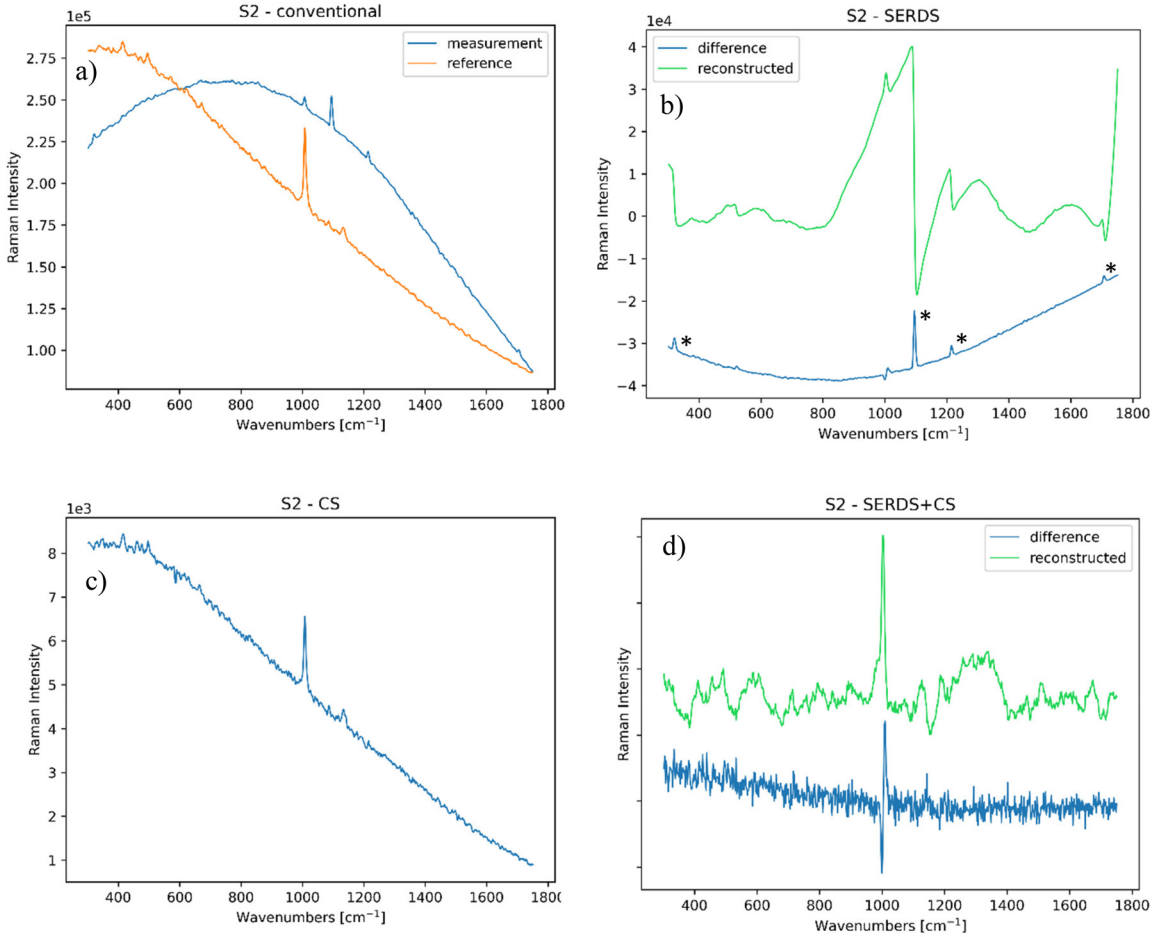

Fig. 4 (a) Conventional Raman spectrum of the gypsum sample, compared to the reference baseline (S/N = 0.24); (b) SERDS measurement of the same sample (S/N = 0.1); (c) CS measurement of the same sample (S/N = 19); and (d) SERDS + CS measurement of the same sample (S/N = 17). All bands highlighted with (*) are artefacts or background interferences.

sample. Also in this scenario, this interfering background was then effectively suppressed with the combined SERDS + CS measurement (Fig. 4d).

Paper (S3). Paper is often found in many contemporary artworks or collages and is used as a support for historical documents, manuscripts or some paintings. It usually possesses a weak Raman signal of cellulose and sometimes also Raman bands of calcite (where present as a whitening agent). In our case, the selected characteristic Raman band of the top layer was a strong calcite peak at 1086 cm^{-1}. This happens to be positioned very closely to the room light band at 1093 cm^{-1}, rendering its detection extremely challenging, and indeed it was the principal reason why both the conventional Raman and SERDS measurements (Fig. 5a and b) could not yield any satisfactory results. In contrast, the charge-shifting and SERDS + CS methods (Fig. 5c and d) were able to clearly remove both the dynamic and static contributions of ambient light. However, even though the latter still provided the Raman signal of calcite, it still possessed a significant degree of interfering background, which renders the charge-shifting measurement shown in Fig. 5c more suitable for interpretation. The reconstructed SERDS spectra contain a considerable degree of artefact features stemming mainly from residual ambient light signal contributions.

SORS measurements

In the second part of the study, we selected layered samples with increasing complexity (considering their scattering efficiency) to evaluate the performance of the combined use of SORS with SERDS and charge-shifting approaches. As mentioned above, these samples are also relevant to the field of cultural heritage, mimicking contemporary art and design materials (plastics) or collages.

PTFE over marble (S4). The first sample consisted of a PTFE layer tape on top of a marble substrate. Both layers possess a high Raman scattering cross section and a low degree of fluorescence interference, with characteristic Raman bands at around 734 cm^{-1} (PTFE, top layer) and 1086 cm^{-1} (calcite – main component of the marble sublayer). Fig. 6a shows the results of conventional SORS measurement at 0 and 2 mm spatial offsets: the PTFE signal is appreciable and decreases with increasing offset, as expected, but the calcite band is

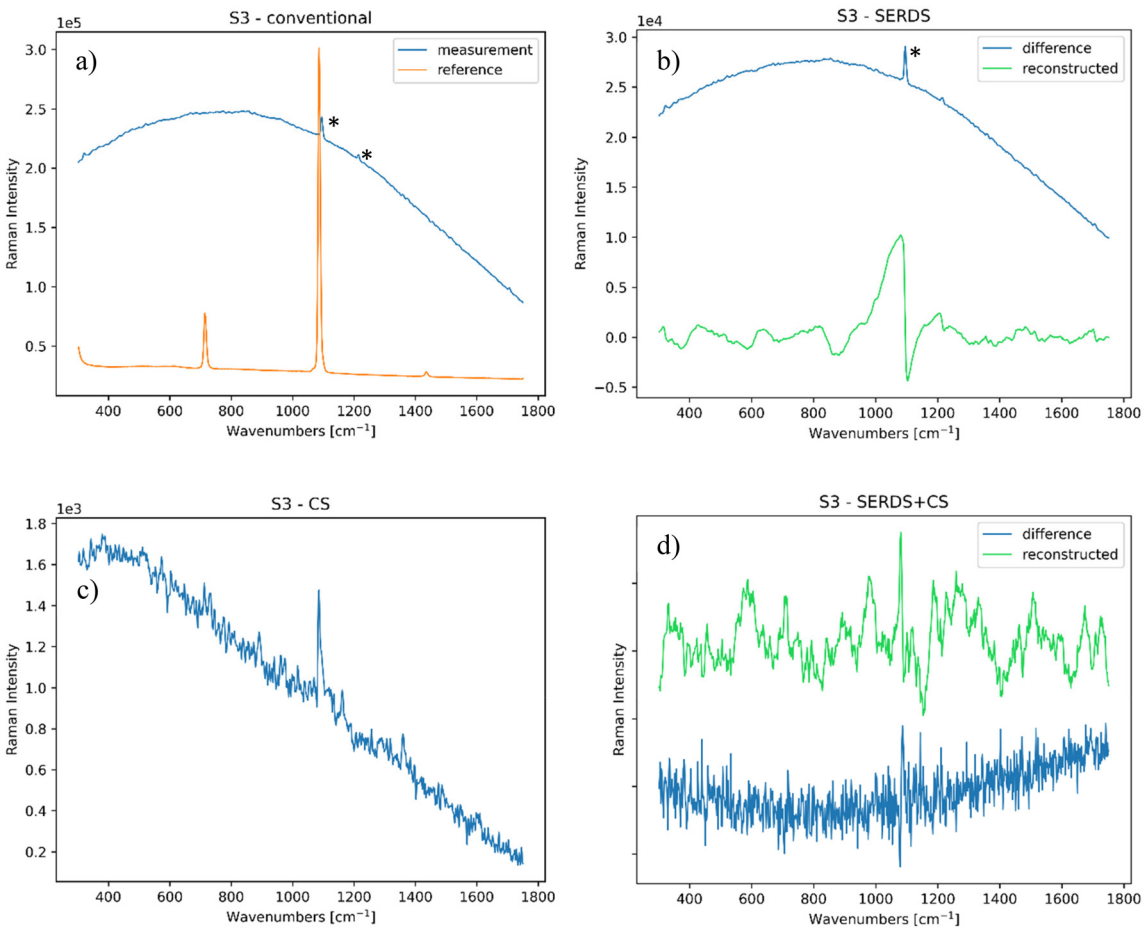

Fig. 5 (a) Conventional Raman spectrum of the paper sample, compared to the reference (S/N = 0.05); (b) SERDS measurement of the same sample (S/N = 0.03); (c) CS measurement of the same sample (S/N = 6.9); and (d) SERDS + CS measurement of the same sample (S/N = 3). All bands highlighted with (*) are artefacts or background interferences.

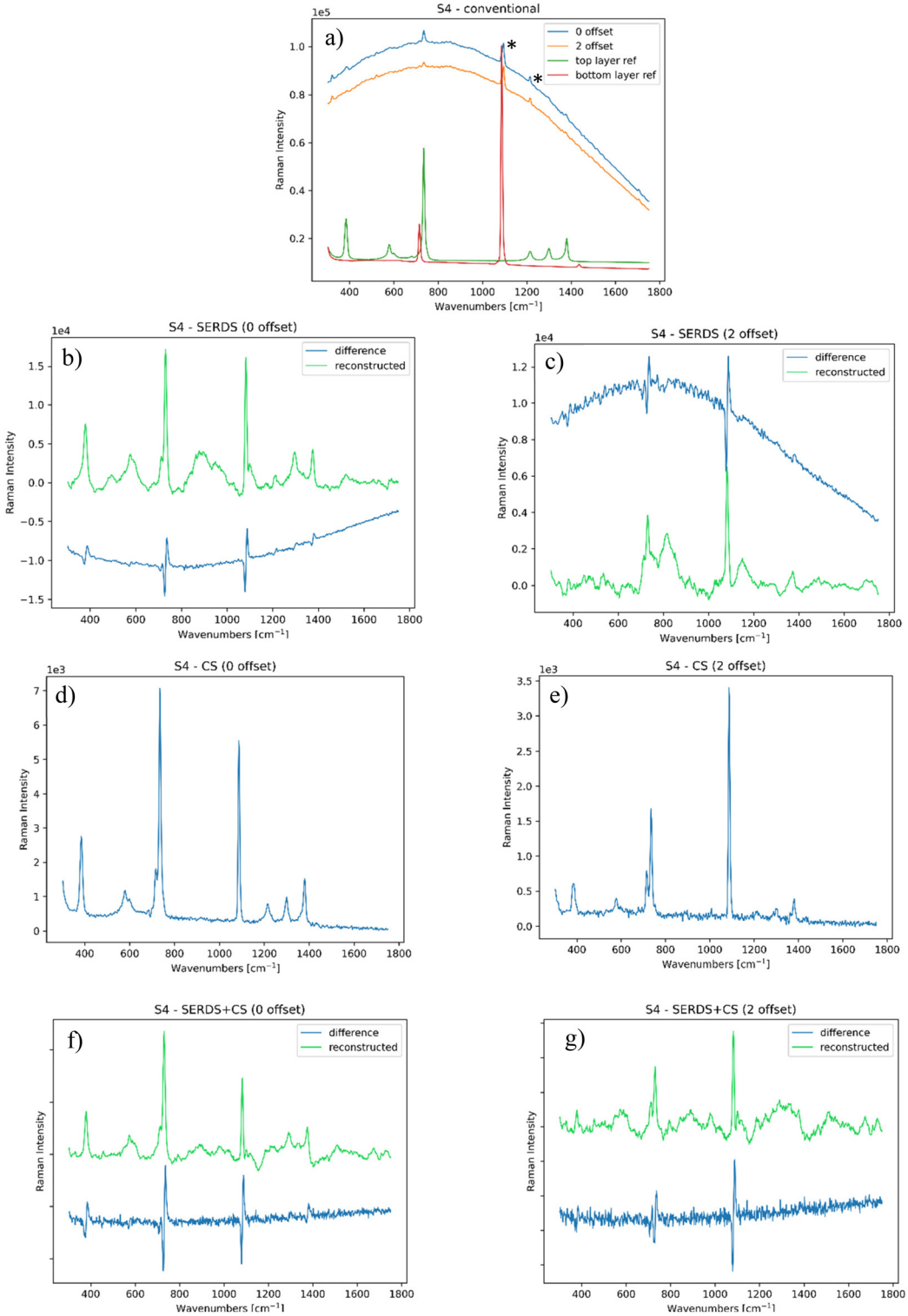

Fig. 6 (a) Conventional SORS Raman spectrum of PTFE over marble, compared to the reference (S/N = 0.38); SERDS measurement of the same sample at (b) 0 and (c) 2 mm offset (S/N = 17); charge-shifting measurement of PTFE over marble at (d) 0 and (e) 2 mm offset (S/N = 62); SERDS + CS analyses of the same sample at (f) 0 and (g) 2 mm offset (S/N = 30).

once again masked by the room light emission line at 1093 cm^{-1}. SERDS-SORS measurements at 0 and 2 mm offset, shown in Fig. 6b and c, evidence the SORS effect, where the top layer signal (PTFE, 734 cm^{-1}) decreases faster than the sublayer signal as the offset increases, leading to a predominance of the bottom layer signal (calcite, 1086 cm^{-1}). Thanks to the low fluorescence and high Raman scattering cross sections of the layers, the Raman bands are clearly visible also at

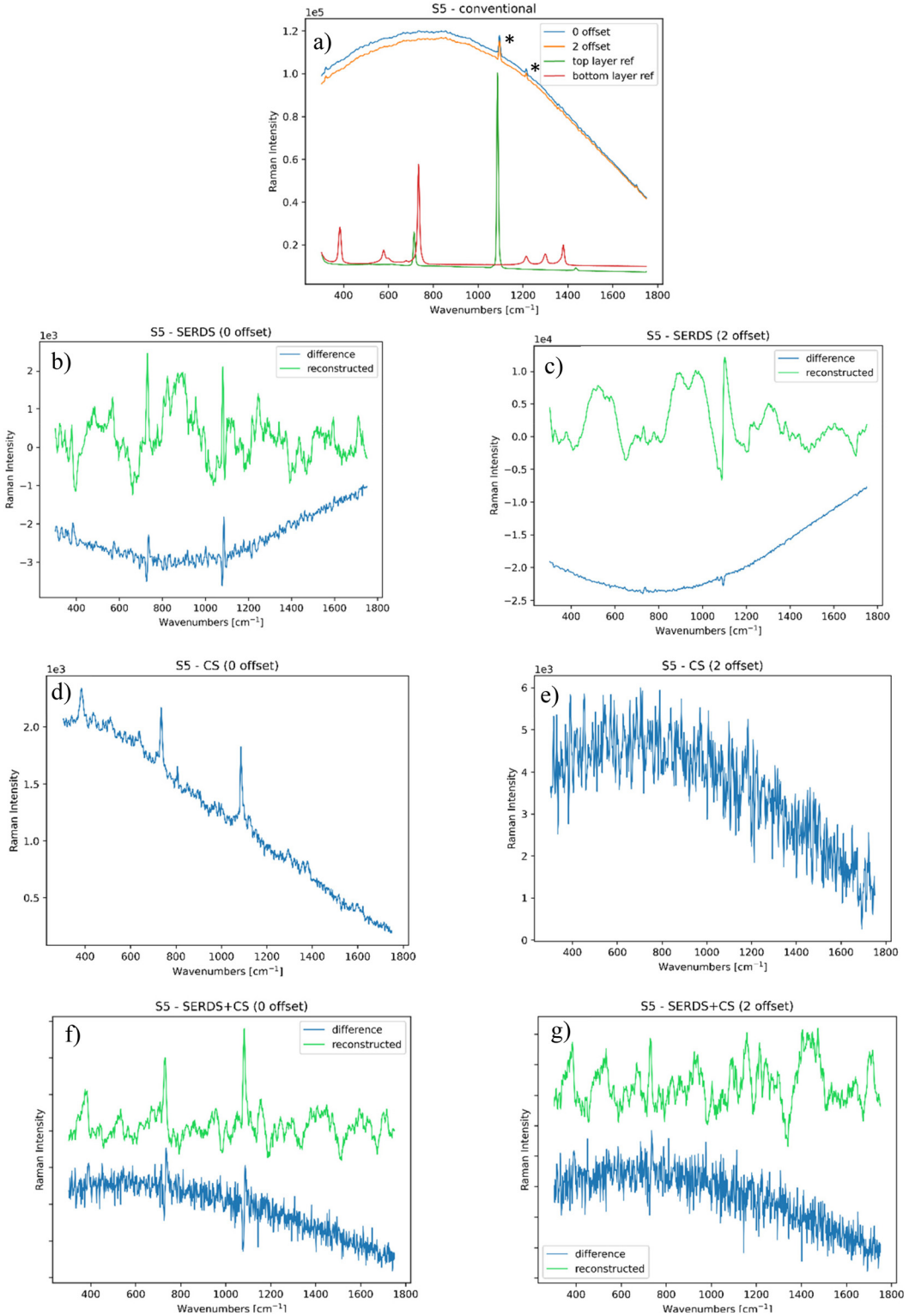

Fig. 7 (a) Conventional SORS Raman spectrum of paper over PTFE, compared to the reference (S/N = 0.05); SERDS measurement of the same sample at (b) 0 and (c) 2 mm offset (S/N = 0.22); charge-shifting measurement of paper over PTFE at (d) 0 and (e) 2 mm offset (S/N = 6); SERDS + CS analyses of the same sample at (f) 0 and (g) 2 mm offset (S/N = 1.3).

this stage, even though the background interference still has a significant impact on the result.

CS measurements (shown in Fig. 6d and e) removed most of the dynamic ambient light contributions and given the nature of the sample there is no significant fluorescence contribution present. The spectra also showed an appreciable SORS effect. In comparison, SERDS + CS measurements (see Fig. 6f and g) yielded poorer results. This is attributed to the fact that the contribution of fluorescence from the sample was relatively low, making SERDS redundant and consequently the deployment of SERDS + CS only added an extra noise under our specific acquisition conditions, as noted earlier.[17]

Paper over PTFE (S5). Further increasing the complexity of the samples, S3 was placed on top of a PTFE block. Fig. 7a shows the conventional measurement compared with the reference spectra of individual layers: both the characteristic bands of PTFE (734 cm^{-1}) and calcite (1086 cm^{-1}) are not visible at a 0 or 2 mm offset. SERDS measurement at 0 offset (Fig. 7b) was able to detect the Raman bands of both layers, while in the 2 mm offset measurement (Fig. 7c) both Raman bands were masked by background light interference.

Similarly, the 0 mm offset CS and SERDS + CS measurements (Fig. 7d and f) were able to detect the Raman bands of the compounds involved, with the former yielding a higher quality spectrum. The outcome with the 2 mm offset was however different as in this case the charge-shifting method alone (Fig. 7e) was not able to retrieve any signal from the top or bottom layer, possibly compounded by photon absorption within the paper. In contrast, the SERDS + CS approach detected the PTFE signal of the subsurface, removing effectively the calcite band coming from the top layer (Fig. 7g). In this scenario, the full capability of the combined SERDS and charge-shifting method was essential to render a satisfactory result. The combined use of SORS, SERDS and CS readout approaches was capable of non-invasive probing of the inner layers of a sample while rejecting any static and dynamic interfering contributions. As previously mentioned, the amount of noise-like features in these spectra are related to the necessity of setting of the charge-shifting measurements out of its optimal regime, in order to obtain results comparable to those of other techniques.

Conclusions

The challenges presented by *in situ* field measurements in heritage science are numerous, stemming from both ambient light contributions and sample fluorescence, and these are often combined creating specific, highly challenging scenarios. Given the necessity to perform accurate *in situ* measurements while rejecting any signals that differ from Raman signals of interest, we demonstrated that the synergy between SERDS and charge-shifting technologies, where the former is able to mitigate fluorescence interference and the latter allows us to deal with varying ambient light, is highly beneficial in dealing with such scenarios.

When the sample is highly fluorescent and there is no dynamic variation of the ambient light, SERDS proved to be the most effective approach. In this situation, the charge-shifting approach was not able to deal with sample fluorescence as SERDS. However, when the background evolved dynamically, the employment of charge-shifting was therefore fundamentally important. We proved that through this combination of techniques it is possible to obtain promising results when simulating highly challenging *in situ* conditions, such as varying cloud coverage or shadows projected onto the collection side of the instrument or the variation of artificial room light. Quality of the spectra can be further improved, especially considering that the charge-shifting instrument worked outside its optimum regime. We have also shown that these techniques can be combined with SORS paving a way for the non-invasive investigations of the subsurface components of materials *in situ* while simultaneously rejecting ambient light and fluorescence interfering contributions.

Data availability

Data are openly available in a Mendeley Data repository.

Lux, Alberto; Conti, Claudia; Botteon, Alessandra; Mosca, Sara; Matousek, Pavel (2024), *"CS paper", Mendeley Data, V1*, **https://doi.org/10.17632/6fdxbc8h83.1**.

Conflicts of interest

There are no conflicts of interest to declare.

References

1 K. Shin and H. Chung, Wide area coverage Raman spectroscopy for reliable quantitative analysis and its applications, *Analyst*, 2013, **138**(12), 3335, DOI: **10.1039/c3an36843b**.
2 W. J. Olds, E. Jaatinen, P. Fredericks, B. Cletus, H. Panayiotou and E. L. Izake, Spatially offset Raman spectroscopy (SORS) for the analysis and detection of packaged pharmaceuticals and concealed drugs, *Forensic Sci. Int.*, 2011, **212**, 69–77.
3 P. W. Loeffen, G. Maskall, S. Bonthron, M. Bloomfield, C. Tombling and P. Matousek, Chemical and explosives point detection through opaque containers using spatially offset Raman spectroscopy (SORS), Chem. Biol. Radiol. Nucl. Explos. Sens. XII, 2011, 8018: 80181E. DOI: **10.1117/12.882126**.
4 Z. Movasaghi, S. Rehman and I. U. Rehman, Raman Spectroscopy of Biological Tissues, *Appl. Spectrosc. Rev.*, 2007, **42**(5), 493–541, DOI: **10.1080/05704920701551530**.
5 F. Korinth, T. A. Shaik, J. Popp and C. Krafft, Assessment of shifted excitation Raman difference spectroscopy in highly fluorescent biological samples, *Analyst*, 2021, **146**(22), 6760–6767, DOI: **10.1039/d1an01376a**.

6 D. I. Ellis, R. Eccles, Y. Xu, J. Griffen, H. Muhamadali, P. Matousek, *et al.*, Through-container, extremely low concentration detection of multiple chemical markers of counterfeit alcohol using a handheld SORS device, *Sci. Rep.*, 2017, **7**(1), 12082, DOI: **10.1038/s41598-017-12263-0**.

7 C. Conti, A. Botteon, C. Colombo, M. Realini and P. Matousek, Fluorescence suppression using micro-scale spatially offset Raman spectroscopy, *Analyst*, 2016, **141**, 5374–5381, DOI: **10.1039/c6an00852f**.

8 K. Sowoidnich and H.-D. Kronfeldt, Fluorescence Rejection by Shifted Excitation Raman Difference Spectroscopy at Multiple Wavelengths for the Investigation of Biological Samples, *ISRN Spectrosc.*, 2012, **2012**, 1–11, DOI: **10.5402/2012/256326**.

9 K. Sowoidnich, M. Oster, K. Wimmers, M. Maiwald and B. Sumpf, Shifted excitation Raman difference spectroscopy as enabling technique for the analysis of animal feedstuff, *J. Raman Spectrosc.*, 2021, **52**(8), 1418–1427, DOI: **10.1002/jrs.6140**.

10 J. Zhao, M. M. Carrabba and F. S. Allen, Automated Fluorescence Rejection Using Shifted Excitation Raman Difference Spectroscopy, *Appl. Spectrosc.*, 2002, **56**(7), 834–845, DOI: **10.1366/000370202760171491**.

11 A. P. Shreve, N. J. Cherepy and R. A. Mathies, Effective Rejection of Fluorescence Interference in Raman Spectroscopy Using a Shifted Excitation Difference Technique, *Appl. Spectrosc.*, 1992, **46**(4), 707–711, DOI: **10.1366/0003702924125122**.

12 B. Sumpf, M. Maiwald, A. Müller, J. Fricke, P. Ressel, F. Bugge, *et al.*, Comparison of two concepts for dual-wavelength DBR ridge waveguide diode lasers at 785 nm suitable for shifted excitation Raman difference spectroscopy, *Appl. Phys. B: Lasers Opt.*, 2015, **120**(2), 261–269, DOI: **10.1007/s00340-015-6133-x**.

13 M. Maiwald, B. Eppich, J. Fricke, A. Ginolas, F. Bugge, B. Sumpf, *et al.*, Dual-Wavelength Y-Branch Distributed Bragg Reflector Diode Laser at 785 Nanometers for Shifted Excitation Raman Difference Spectroscopy, *Appl. Spectrosc.*, 2014, **68**(8), 838–843, DOI: **10.1366/13-07331**.

14 P. Strobbia, V. Cupil-Garcia, B. M. Crawford, A. M. Fales, T. J. Pfefer, Y. Liu, *et al.*, Accurate in vivo tumor detection using plasmonic-enhanced shifted-excitation Raman difference spectroscopy (SERDS), *Theranostics*, 2021, **11**(9), 4090–4102, DOI: **10.7150/thno.53101**.

15 K. Sowoidnich, M. Towrie and P. Matousek, Lock-in detection in Raman spectroscopy with charge-shifting CCD for suppression of fast varying backgrounds, *J. Raman Spectrosc.*, 2019, **50**(7), 983–995, DOI: **10.1002/jrs.5597**.

16 K. Sowoidnich, M. Towrie, M. Maiwald, B. Sumpf and P. Matousek, Shifted Excitation Raman Difference Spectroscopy with Charge-Shifting Charge-Coupled Device (CCD) Lock-In Detection, *Appl. Spectrosc.*, 2019, **73**(11), 1265–1276, DOI: **10.1177/0003702819859352**.

17 S. Mosca, K. Sowoidnich, M. Mehta, W. H. Skinner, B. Gardner, F. Palombo, *et al.*, 10 kHz Shifted-Excitation Raman Difference Spectroscopy with Charge-Shifting Charge-Coupled Device Read-Out for Effective Mitigation of Dynamic Interfering Backgrounds, *Appl. Spectrosc.*, 2023, **77**(6), 569–582, DOI: **10.1177/00037028231167441**.

18 D. Cebeci-Maltaş, P. Wang, M. A. Alam, R. Pinal and D. Ben-Amotz, Photobleaching profile of Raman peaks and fluorescence background, *Eur. Pharm. Rev.*, 2017, **22**(6), 18–21.

19 P. Matousek, I. P. Clark, E. R. C. Draper, M. D. Morris, A. E. Goodship, N. Everall, *et al.*, Subsurface probing in diffusely scattering media using spatially offset Raman spectroscopy, *Appl. Spectrosc.*, 2005, **59**(4), 393–400, DOI: **10.1366/0003702053641450**.

20 S. Mosca, C. Conti, N. Stone and P. Matousek, Spatially offset Raman spectroscopy, *Nat. Rev. Methods Primers*, 2021, **1(1)**, DOI: **10.1038/s43586-021-00019-0**.

21 S. Mosca, P. Dey, M. Salimi, B. Gardner, F. Palombo, N. Stone, *et al.*, Spatially Offset Raman Spectroscopy - How Deep?, *Anal. Chem.*, 2021, **93**(17), 6755–6762, DOI: **10.1021/acs.analchem.1c00490**.

22 A. Lux, M. Realini, A. Botteon, M. Maiwald, A. Müller, B. Sumpf, *et al.*, Advanced portable micro-SORS prototype coupled with SERDS for heritage science, *Analyst*, 2024, **149**(8), 2317–2327, DOI: **10.1039/d3an02215c**.

23 B. Sumpf, A. Müller and M. Maiwald, Tailored diode lasers: enabling Raman spectroscopy in the presence of disturbing fluorescence and background light, in *Proc. SPIE 10894, Plasmonics in Biology and Medicine XVI*, 2019, 1089411, DOI: **10.1117/12.2507425**.

24 S. Mosca, M. Mehta, W. H. Skinner, B. Gardner, F. Palombo, N. Stone, *et al.*, Active Surface-Enhanced Raman Spectroscopy (SERS): A Novel Concept for Enhancing Signal Contrast in Complex Matrices Using External Perturbation, *Appl. Spectrosc.*, 2024, 1–8, DOI: **10.1177/00037028241267898**.

25 P. Matousek, M. Towrie and A. W. Parker, Simple reconstruction algorithm for shifted excitation Raman difference spectroscopy, *Appl. Spectrosc.*, 2005, **59**(6), 848–851, DOI: **10.1366/0003702054280757**.